AIP The Journal of Chemical Physics

Benzene analogues of (quasi-)planar M@BnHn compounds (M = V−, Cr, Mn+): A theoretical investigation

Lifen Li, Chang Xu, Baokang Jin, and Longjiu Cheng

Citation: J. Chem. Phys. **139**, 174310 (2013); doi: 10.1063/1.4827517
View online: http://dx.doi.org/10.1063/1.4827517
View Table of Contents: http://jcp.aip.org/resource/1/JCPSA6/v139/i17
Published by the AIP Publishing LLC.

THE JOURNAL OF CHEMICAL PHYSICS **139**, 174310 (2013)

Benzene analogues of (quasi-)planar $M@B_nH_n$ compounds ($M = V^-$, Cr, Mn^+): A theoretical investigation

Lifen Li (李丽芬), Chang Xu (徐畅), Baokang Jin (金葆康), and Longjiu Cheng (程龙玖)[a)]
Department of Chemistry, Anhui University, Hefei, Anhui 230039, People's Republic of China

(Received 18 July 2013; accepted 16 October 2013; published online 5 November 2013)

The stability of $M@B_nH_n$ ($M = V^-$, Cr, Mn^+; $n = 5$–8) is investigated by density functional theory. For $n = 6$–8, the isomers possess (quasi-)planar local minima showed by geometry optimization at TPSSh/6-311+G** level. All the optimized structures are thermodynamics stable according to the large HOMO-LUMO gap, binding energy, vertical ionization potential, and vertical electron affinity analysis. The peripheral and central atomic radius fit each other best at $n = 7$ confirmed by the variation of the binding energy values. The availability of d atom orbitals in M for participation in the π-delocalized bonding with the peripheral ring leads to the aromaticity of the (quasi-)planar structures and makes them the benzene analogues. This work establishes firmly the metal-doped borane rings as a new type of aromatic molecule. © *2013 AIP Publishing LLC*. [http://dx.doi.org/10.1063/1.4827517]

I. INTRODUCTION

Boron and boron-based clusters have attracted much attention in the past 20 years owning to their interesting physical and chemical properties.[1–32] Experimental and theoretical studies over the last decades have demonstrated that positively charged boron clusters are shown to become 3D at B_{16}^+,[33–36] while negatively charged and neutral boron clusters are still planar at B_{23}^- and B_{19},[37–49] respectively, except for B_{14}.[50] Two types of delocalized bonding – the in-plane σ and the out-of-plane π bonding are found in the planar boron clusters, each of which follows the $(4n + 2)$ Huckel rule for aromaticity. The delocalized bonding results in multiple aromaticity and enhances the stability of the planar clusters, such as molecular wheel-type clusters D_{7h} $B@B_7^{2-}$ and D_{8h} $B@B_8^-$.[51] Those novel bonding situations suggest that other atoms with appropriate valence electrons numbers and sizes may be able to substitute the central boron atom to produce $M@B_n$-type clusters. In 2007, Merion and co-workers[52] designed sets of boron rings enclosing planar hypercoordinate group 14 elements ($AB_n^{(n-8)}$; A = group 14 element; $n = 6$–10), which illustrated that the ring and the center atomic radii must match and the radial/π electron delocalization determines the stability of the hypercoordinate molecules. Besides, joint experimental and theoretical study, a series of metal-doped B_n clusters is reported by Boldyrev-Wang.[53–64] Formation of ionic bonds in Al-doped boron clusters was observed for AlB_n^-($n = 7$–11) clusters and Al does not participate in delocalized bonding.[56,60,63] However, doping boron rings with transition metals are found thermodynamically stable metal-centered aromatic compounds, which are wheel-type structures in perfect symmetry, such as neutral, $Rh@B_9$ and $Ir@B_9$ clusters,[61] and anionic, $Co@B_8^-$, $Ru@B_9^-$,[58] $Ta@B_{10}^-$, $Nb@B_{10}^-$,[62] $Fe@B_8^-$, $Fe@B_9^-$,[57] VB_{10}^-.[59] Transition-metal atoms are better suited for the central position in the $M@B_n$ clusters, because these metals favor participation in delocalized bonding at the center over localized bonding at the periphery.

Lots of hydrogenated small boron clusters were reported;[46,65–67] however, most boron hydrides adopt three-dimensional aromatic structures. In 2009, Yu and co-workers[68] presented a borane cation $[B_6H_5]^+$ in D_{5h} symmetry, in which all the B atoms are sp^2 hybridization and the p_z atom orbitals of those B atoms interact with each other. Recently, we also studied the geometric and electronic structures of $X@B_nH_n$ ($X = Be, B^+$; $n = 5$–8).[69] Compared to C_6H_6, the framework of the hydrogenated cyclic boron (B_nH_n) is formed by n B–H bonds and n B–B bonds, and the overlapped p_z orbitals of the peripheral boron (B_{per}) are empty due to the electron deficiency of boron. Thus, according to our design, the electronic number occupied the empty orbitals is decided on the valence electronic number of the center atom. Both of Be and B^+ have two valence electrons, which can enter into the empty p_z atom orbitals of the peripheral boron and satisfy the Huckle aromatic rule.

Although $M@B_n$ and borane clusters are paid much attention, the $M@B_nH_n$ clusters are less investigated. In this work, we adopt density functional theory (DFT) method to investigate the structures and properties of $M@B_nH_n$ ($M = V^-$, Cr, Mn^+; $n = 5$–8) clusters. Each of the V^-, Cr, and Mn^+ has six valence electrons, which would occupy the empty overlapped p_z orbitals in our assumption. The results show that the (quasi-)planar $M@B_nH_n$ are stale at $n = 6$–8, and $[V@B_7H_7]^-$ has a planar local minimum in D_{7h} symmetry. Besides, $M@B_nH_n$ ($X = V^-$, Cr, Mn^+; $n = 6$–8) are found to be benzene analogues, which confirmed our assumption, according to the electronic structure analysis.

II. COMPUTATIONAL DETAILS

The geometries of $M@B_nH_n$ ($M = V^-$, Cr, Mn^+; $n = 5$–8) are optimized by using the TPSSh functional.[70]

[a)] Author to whom correspondence should be addressed. Electronic mail: clj@ustc.edu. Tel./Fax: +86-551-5107342.

0021-9606/2013/139(17)/174310/7/$30.00

The structures of Cr@B_nH_n (n = 5–7) are investigated using the method combining the genetic algorithm (GA) with DFT implemented in our group.[71–74] The optimization and the calculations of the energies and HOMO-LUMO gaps are performed at the TPSSh/6-311+G** level, and the natural population analysis is performed at the TPSSh/6-311G* level. In the adaptive natural density partitioning (AdNDP) analysis procedure, the 6-31G* and lanl2dz basis sets are employed for ligands and transition metals, respectively. The TPSSh functional was proven to give reasonably accurate energetic properties of boron and boron-based clusters.[3,50,72,75,76] To confirm the stability of structures, we analyze the vibrational frequencies, and the results show that all isomers for each cluster are true local minima. The binding energy of the compound is defined as $E_b = E$ (M@B_nH_n) $-$ E (M) $-E$ (B_nH_n). Then, the vertical ionization potential (VIP) of [V@B_nH_n]$^-$ is calculated as E (V@B_nH_n) $-$ E ([V@B_nH_n]$^-$), VIP of Cr@B_nH_n is E ([Cr@B_nH_n]$^+$) $-$ E (Cr@B_nH_n), the vertical electron affinity (VEA) of Cr@B_nH_n is E (Cr@B_nH_n) $-$ E ([Cr@B_nH_n]$^-$), and VEA of [Mn@B_nH_n]$^+$ is E ([Mn@B_nH_n]$^+$) $-$ E (Mn@B_nH_n). All calculations are carried out by using the GAUSSIAN 09 package.[77]

III. RESULTS AND DISCUSSION

We optimize M@B_nH_n (M = V$^-$, Cr, Mn$^+$; n = 5–8) at TPSSh/6-311+G** level started from D_{nh} symmetry. Figure 1 plots the local minima of M@B_nH_n (M = V$^-$, Cr, Mn$^+$; n = 5–8) from two sides. The binding energy, energy gap, VEA, VIP, and nucleus-independent chemical shifts (NICS) value[78] above the molecular plane 1 Å and the natural charge of M@B_nH_n and benzene are listed in Table I.

A. Geometry structures

The optimized M@B_nH_n (M = V$^-$, Cr, Mn$^+$; n = 5–8) structures distort seriously at n = 5 and possess (quasi-)planar motifs at n = 6–8. [V@B_6H_6]$^-$ is a bowl-like structure in C_{6v} symmetry, in which the center V atom has a 0.70 Å outstand to the plane composed by peripheral B atoms. [V@B_7H_7]$^-$ has a planar motif with a high symmetry in D_{7h}. It becomes a saddle-shaped structure in D_{2d} symmetry at n = 8. Cr@B_nH_n are bowl-like in C_{6v} and C_{7v} symmetry at n = 6 and n = 7, so do [Mn@B_nH_n]$^+$. The Cr has a 0.57 Å and a 0.20 Å outstand to the plane of the B atoms for n = 6 and n = 7, respectively, while those for Mn are 0.51 Å and 0.31 Å. Cr@B_8H_8

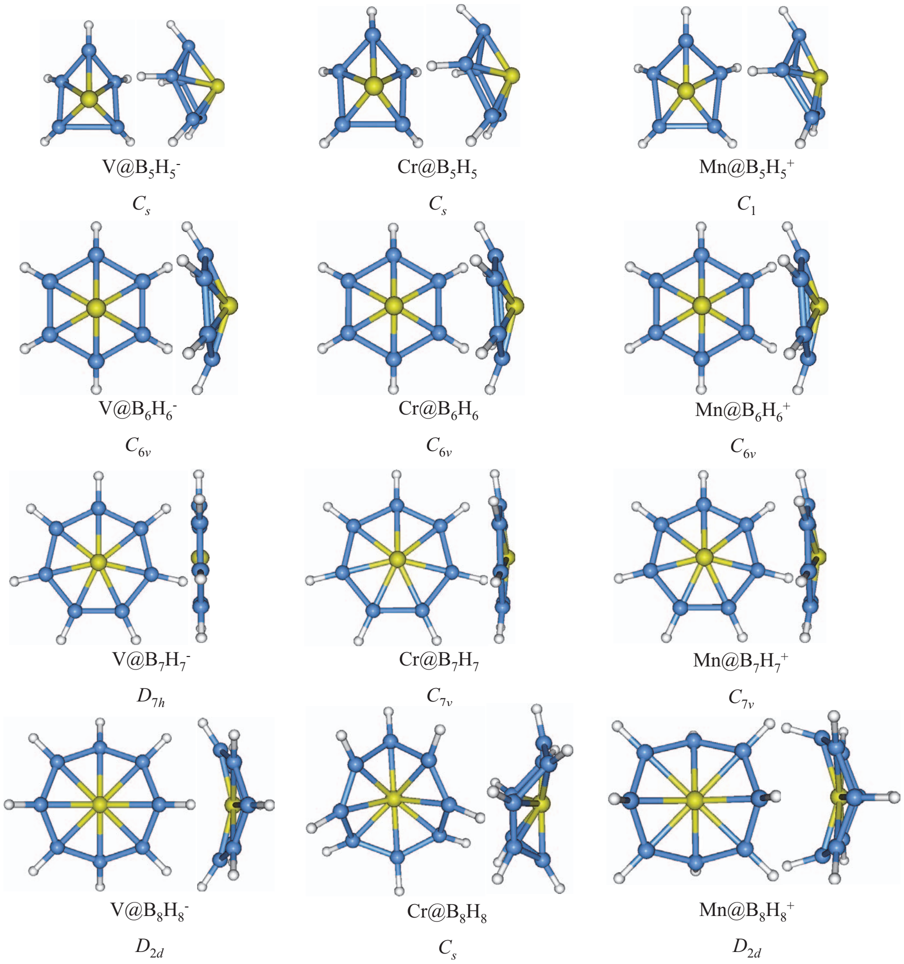
V@$B_5H_5^-$ C_s
Cr@B_5H_5 C_s
Mn@$B_5H_5^+$ C_1
V@$B_6H_6^-$ C_{6v}
Cr@B_6H_6 C_{6v}
Mn@$B_6H_6^+$ C_{6v}
V@$B_7H_7^-$ D_{7h}
Cr@B_7H_7 C_{7v}
Mn@$B_7H_7^+$ C_{7v}
V@$B_8H_8^-$ D_{2d}
Cr@B_8H_8 C_s
Mn@$B_8H_8^+$ D_{2d}

FIG. 1. Local minima of M@B_nH_n for M = V$^-$, Cr, Mn$^+$ and n = 5–8. The symmetry is labeled in figure (two sides of views are given): H-white, B-blue, and M-yellow.

TABLE I. Energy gap (eV) and NICS(1) values (ppm) for M@B_nH_n (M = V^-, Cr, Mn^+; n = 6–8) and benzene, binding energy (eV) and natural charge (|e|) of the metals for M@B_nH_n (M = V^-, Cr, Mn^+; n = 6–8), vertical ionization potential (eV) for M@B_nH_n (M = V^-, Cr; n = 6–8) and benzene, vertical electron affinity (eV) for M@B_nH_n (M = Cr, Mn^+; n = 6–8) and benzene at TPSSh/6-311+G** level.

	ΔE_{HL}	E_b	VIP	VEA	NICS(1)	q_M
$[V@B_6H_6]^-$	2.85	13.38	2.96		– 58.40	+0.37
$[V@B_7H_7]^-$	3.12	15.95	4.15		– 40.28	+0.63
$[V@B_8H_8]^-$	2.51	15.42	3.74		– 43.28	+0.93
$Cr@B_6H_6$	3.04	8.65	8.47	2.28	– 85.12	+0.35
$Cr@B_7H_7$	2.55	10.66	9.02	3.40	– 98.89	+0.71
$Cr@B_8H_8$	2.36	8.14	8.05	3.57	– 22.22	+0.62
$[Mn@B_6H_6]^+$	3.04	7.50		8.11	– 100.73	+0.43
$[Mn@B_7H_7]^+$	2.02	8.94		9.12	– 135.99	+0.76
$[Mn@B_8H_8]^+$	1.54	4.04		9.15	– 139.87	+0.99
C_6H_6	5.89		9.17	1.33	– 10.19	

has a low symmetry with C_s and $[Mn@B_8H_8]^+$ is in D_{2d} symmetry. The same as $[V@B_7H_7]^-$, both of $Cr@B_8H_8$ and $[Mn@B_8H_8]^+$ are saddle-shaped.

To verify whether the planar structures are the global minimum ones, we performed unbiased global search on the potential energy surface of CrB_nH_n (n = 5–7) using the GA-DFT method, and the low-energy isomers are plotted in Figure 2. The unbiased global optimization confirms that the quasi-planar $Cr@B_6H_6$ and $Cr@B_7H_7$ isomers are the global minimum structures and are 0.27 eV and 0.47 eV lower in energy than the most stable 3D ones, respectively. However, the quasi-planar $Cr@B_5H_5$ structure is much higher in energy than the 3D one (about 1.25 eV) due to the small radius of the B_5H_5 ring. The interesting bonding style between the center transition metal and ligand boron attract our attention due to the electron deficiency of boron and the variety of the bonding styles of the transition metal. We infer there may be delocalized π and/or σ bonds in the molecules. Thus, we focus on only the (quasi-)planar structures hereby instead of the global minimum one.

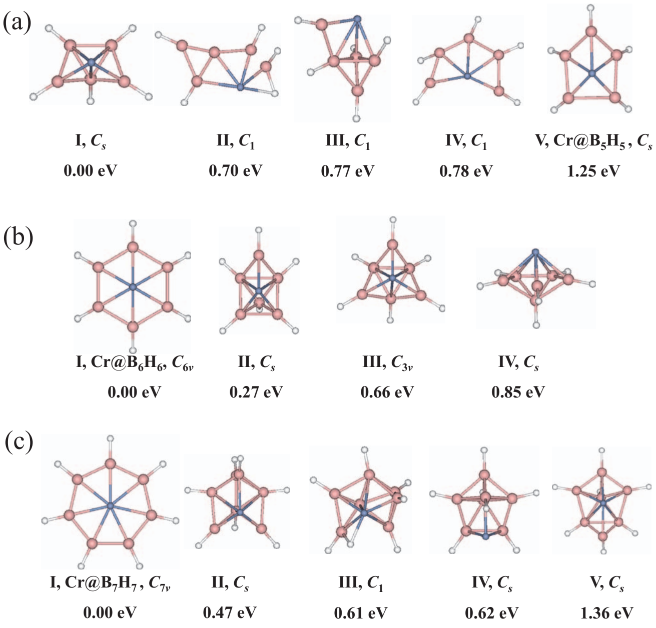

FIG. 2. The low-energy local minima by GA-DFT of (a) CrB_5H_5, (b) CrB_6H_6, and (c) CrB_7H_7 at the TPSSh/6-311+G** level of theory. The structures labeled I correspond to the global minima and II–VI correspond to isomers that are higher in energy; the symmetry and the relative energies in eV are labeled in figure. H-white, B-pink, and Cr-blue.

B. Stability

The stability of those compounds is evaluated theoretically. All the motifs do not have imaginary frequency, that is, all of them are true local minima. The fairly large HOMO-LUMO energy gaps (1.54–3.12 eV) and the binding energy (4.04–15.95 eV) suggest high stability of those systems. Besides, for the same transition metal we calculated, the binding energy is largest at n = 7, which suggest that the peripheral and central atomic radius fit each other most harmoniously at n = 7. Moreover, the VIP values (2.96–4.15 eV) of $[V@B_nH_n]^-$ and the VEA values (2.28–3.57 eV) of $Cr@B_nH_n$ are similar to the VEA values of benzene (1.33 eV), and the VEA values (8.11–9.15 eV) of $[Mn@B_nH_n]^+$ and the VIP values (8.05–9.02 eV) of $Cr@B_nH_n$ are similar to the VIP values of benzene (9.17 eV), which indicates that the anions of $V@B_nH_n$, the natural molecules of $Cr@B_nH_n$, and the cations of $Mn@B_nH_n$ are stable.

C. Aromaticity

M@B_nH_n (M = V^-, Cr, Mn^+; n = 6–8) structures are (quasi-)planar, which is always associated with delocalized electrons. We suggest there may be delocalized electrons in those systems. Since delocalization is always associated with aromaticity, we focus on the aromaticity of those systems. NICS is an easy and efficient criterion to identify aromatic nature. A large negative NICS at the ring center (or inside and above the molecular plane) implies the presence of diamagnetic ring currents. Hereby, we calculate NICS values above the molecular plane (inside of the bowl for the bowl structures) and 1 Å to the center atom (NICS(1)). The NICS(1) values of M@B_nH_n (M = V^-, Cr, Mn^+; n = 6–8) are from −22.22 to −139.87 ppm. Such large negative NICS(1) values indicate that the (quasi-)planar structures are aromatic as a comparison with the NICS(1) value of benzene of −10.19 ppm.

D. Electronic structures

According to the aromaticity of above structures, we infer that there must be delocalized electrons among the clusters. In order to get insight into the delocalized orbital and bonding style of those clusters, canonical molecular orbital (CMO) analysis and AdNDP is adopted. AdNDP is a new theoretical tool developed by Boldyrev group[79,80] for analysis of chemical bonding and has been successfully applied to the analysis of chemical bonding in organic molecules and clusters.[50,72,76,81–84] In the following we pick

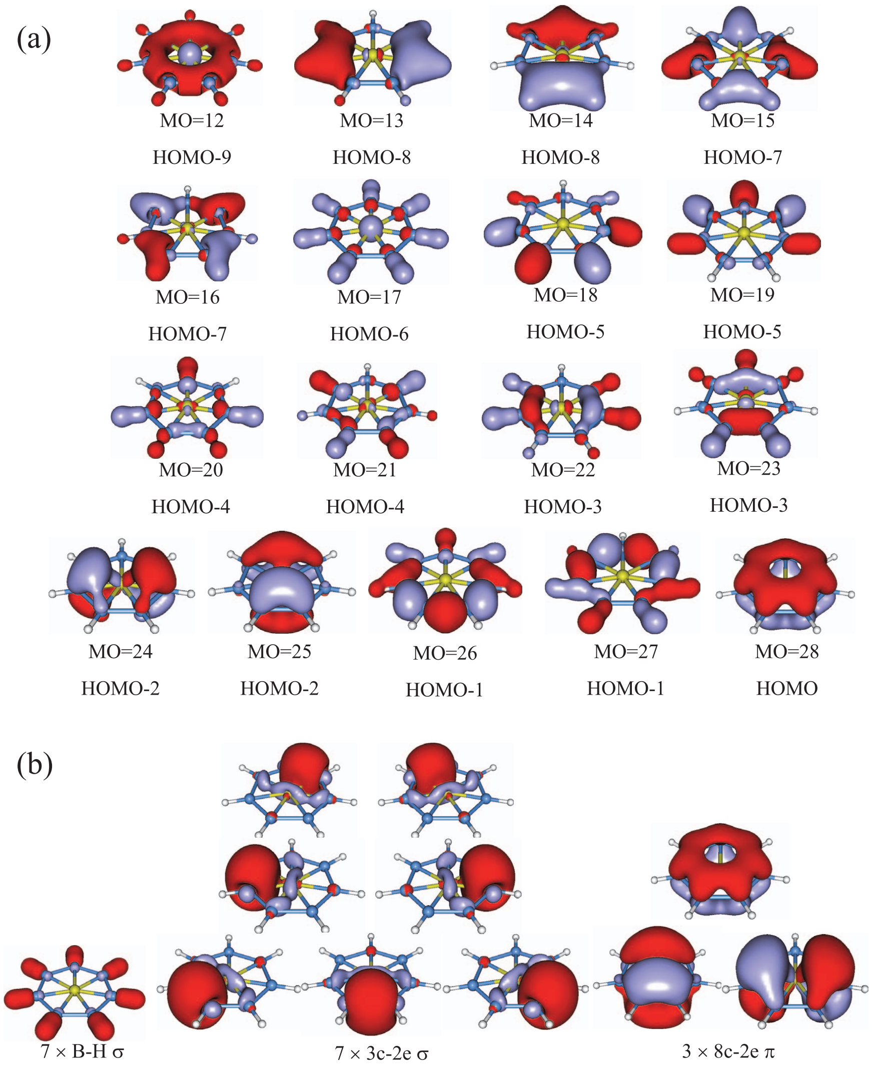

7 × B-H σ
ON=1.94 |e|

7 × 3c-2e σ
ON=1.99 |e|

3 × 8c-2e π
ON=2.00 |e|

FIG. 3. (a) Canonical molecular orbitals and (b) AdNDP localized bonding patterns of $[V@B_7H_7]^-$.

D_{7h} $[V@B_7H_7]^-$, C_{6v} $Cr@B_6H_6$, and D_{2d} $[Mn@B_8H_8]^+$ as examples to discuss their electronic structures.

$[V@B_7H_7]^-$ is planar in D_{7h} symmetry. CMO analysis shows there are three π MOs (MO = 24, 25, and 28 showed in Figure 3(a)). However, it is indistinct to identify other orbitals. In order to gain more insights into the delocalized orbital and bonding style of $[V@B_7H_7]^-$, we present the AdNDP analysis of $[V@B_7H_7]^-$ in Figure 3(b). The AdNDP analysis shows that there are seven localized two-center two-electron (2c-2e) σ-BH bonds, seven delocalized 3c-2e σ-BBV bonds, and three delocalized 8c-2e π bonds with occupy number (ON) of 1.94 |e|, 1.99 |e|, and 2.00 |e|, respectively. On the basis of the above AdNDP analysis, all of the boron atoms are suggested in sp^2 hybridization. One hybridized orbital of B_{per} interacts with the 1*s* orbital of the adjacent H atom, which forms a σ-BH bond; the other two hybridized orbitals of the B_{per} atoms overlap the two hybridized orbitals of V formed by d_{xy} and $d_{x^2-y^2}$ and compose seven 3c-2e σ-BBV bonds. The π MOs are comprised of the p_z orbitals of seven B atoms and the d_{xz} and d_{yz} orbitals are comprised of V atom, which are occupied by the six valence electrons of the center V.

$Cr@B_6H_6$ is bowl-like in C_{6v} symmetry. CMO analysis shows that there are also three π MOs in the molecule (MO = 22, 24, and 25 in Figure 4(a)). The AdNDP analysis (Figure 4(b)) reveals that there are six localized 2c-2e σ-BH bonds, six delocalized 3c-2e σ-BBCr bonds, and three delocalized 7c-2e π bonds (ON = 1.94 |e|, 1.99 |e|, and 2.00 |e|, respectively). The orbital shapes suggest that the three valence electrons of peripheral B form a 2c-2e σ-BH bond and two 3c-2e σ-BBCr bonds, and the six valence electrons of the center Cr delocalized in the molecule occupying the three π MOs, which formed by the d_{z^2}, d_{xz}, and d_{yz} orbital of the center Cr and the p_z orbital of the peripheral B.

$[Mn@B_8H_8]^+$ is saddle-shaped in D_{2d} symmetry. Again, three π MOs are found in the CMO analysis (MO = 29, 30, and 31 in Figure 5(a)). AdNDP analysis of $[Mn@B_8H_8]^+$ is given in Figure 5(b), which suggests that $[Mn@B_8H_8]^+$ possesses eight localized 2c-2e σ-BH bonds, eight delocalized 3c-2e σ-BBMn bonds, and three delocalized 9c-2e π bonds with ON = 1.88 |e|, 1.99 |e|, and 2.00 |e|, respectively. Similarly, one valence electron of the peripheral B contributes to the 2c-2e σ-BH bond and the other two contribute to the two

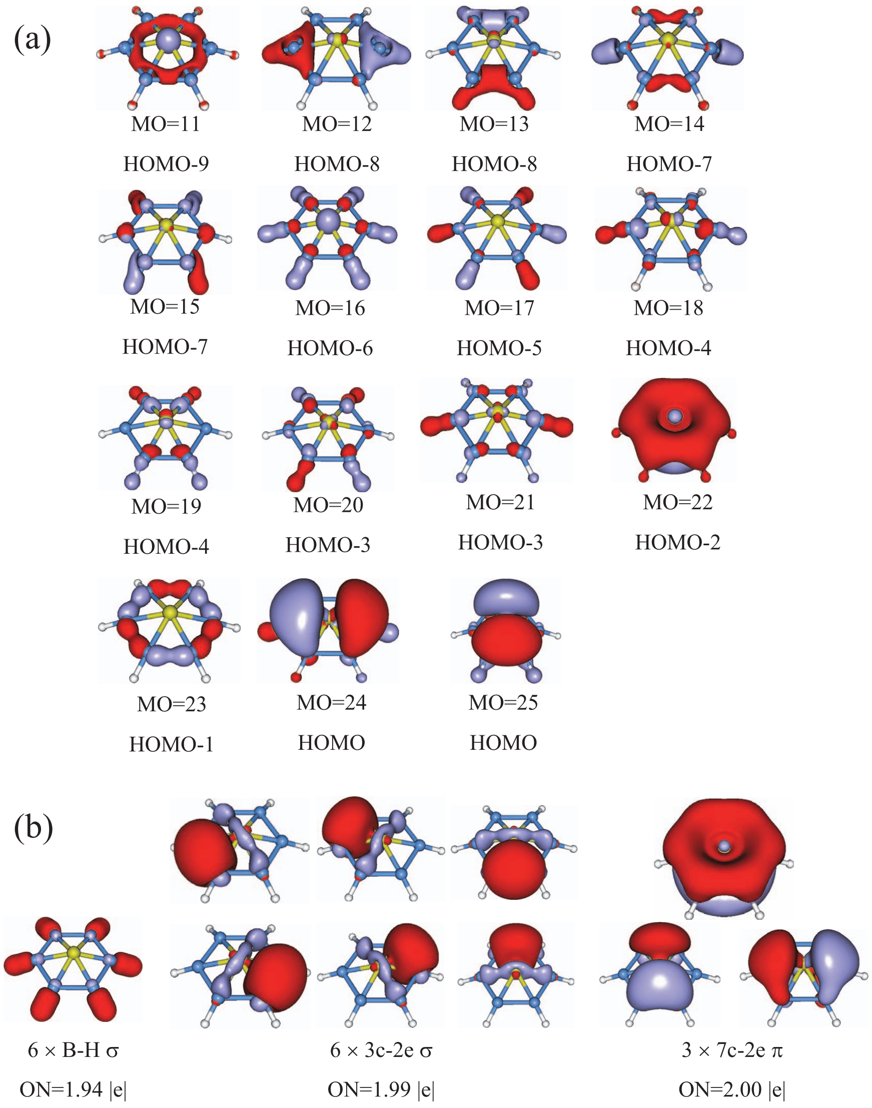

FIG. 4. (a) Canonical molecular orbitals and (b) AdNDP localized bonding patterns of Cr@B_6H_6.

adjacent 3c-2e σ bonds. The π MOs, which store the six valence electrons of the center Mn, are formed by the $d_{x^2-y^2}$, d_{xz}, and d_{yz} orbitals of the center Mn and the p_z orbitals of the peripheral B.

E. Discussion

Based on the analysis above, we can conclude that the bonding type of M@B_nH_n (M = V^-, Cr, Mn^+; $n = 6$–8) are n localized 2c-2e σ-BH bonds, n delocalized 3c-2e σ-BBM bonds, and three delocalized $(n + 1)$c-2e π bonds. All the π MOs are composed by the p_z orbitals of B atoms and the d orbitals of the center atom. However, the involvement d orbitals of the center atom are different for different configurations. For the planar structure ([V@B_7H_7]$^-$), the d_{xz} and the d_{yz} orbitals are involved in the π MOs, which is the same as the planar structure M@B_n.[58,59,62,85–89] While for the bowl-like structures (or the saddle-shaped structures), the d_{z^2} (or $d_{x^2-y^2}$) orbital of the center atoms combined with the d_{xz} and d_{yz} orbitals overlap with the p_z orbitals of the B atoms. The d_{z^2} (or $d_{x^2-y^2}$) orbital involvement with d_{xz} and d_{yz} orbitals are two special bonding manners and much rare between the transition metal and boron. The center metals do not get much positive charges, although the valence electrons of the center transition metal enter into the p_z orbitals of the peripheral B atoms. The center Cr of Cr@B_6H_6, for example, has 0.35 positive charges, according to the natural population analysis. The reason is that the valence electrons of the peripheral B atoms are also entered into the d orbitals of the center metal at the same time, which forms n delocalized 3c-2e σ-BBM bonds. The two kinds bonding types, which are similar to the σ-donation and π-backdonation of organometallic compounds, result in the large binding energies.

IV. CONCLUSION

In summary, we optimize M@B_nH_n (M = V^-, Cr, Mn^+; $n = 5$–8) at TPSSh/6-311+G** level. The clusters distort seriously at $n = 5$. It becomes bowel-like in C_{nv} symmetry at $n = 6$–7, except for [V@B_7H_7]$^-$, which is planar in D_{7h} symmetry. The clusters are saddle-shaped at $n = 8$. The larger energy gap and binding energy support that the structures

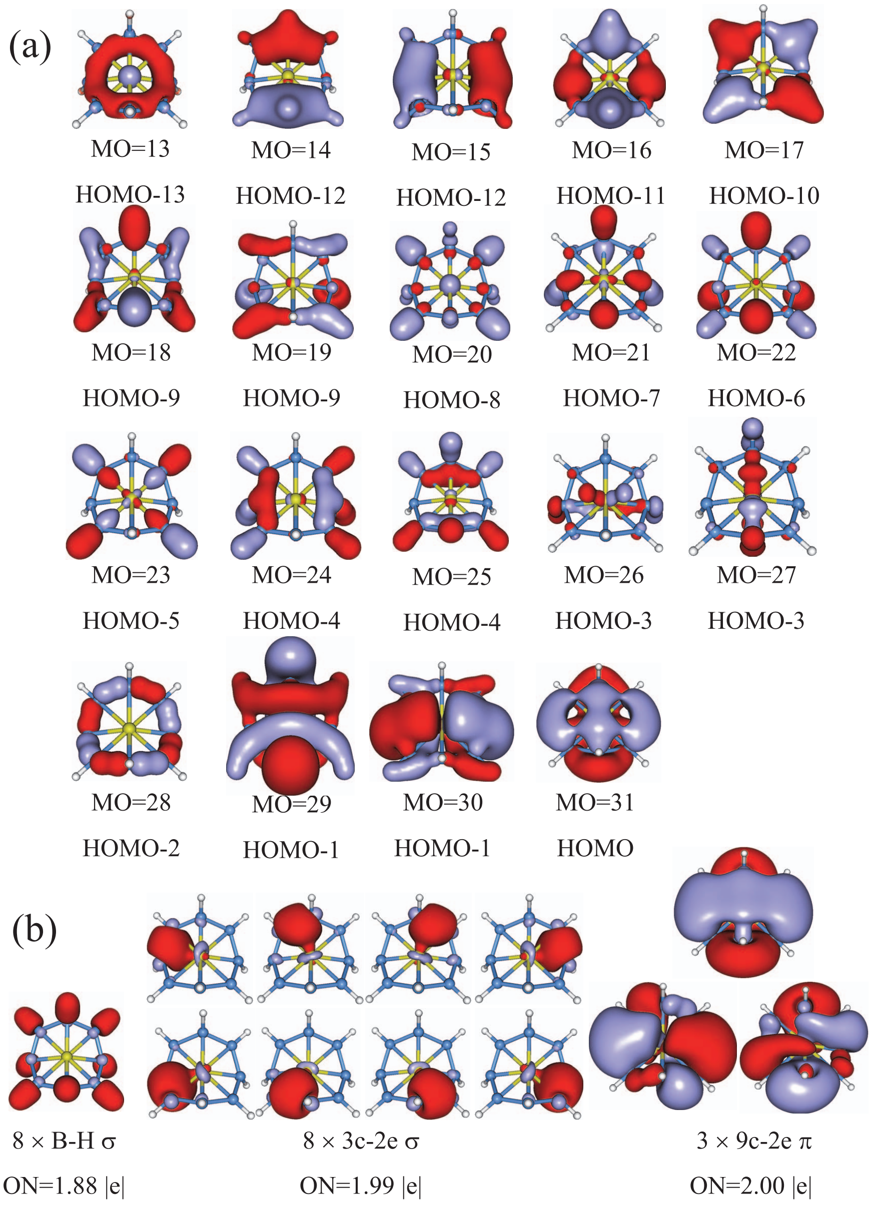

FIG. 5. (a) Canonical molecular orbitals and (b) AdNDP localized bonding patterns of $[\mathrm{Mn@B_8H_8}]^+$.

are stable. The variation of the binding energy values suggests that the peripheral and central atomic radius fit each other best at $n = 7$. NICS values reveal that all of those structures are aromatic, which is confirmed by MO and AdNDP analysis. All of the $\mathrm{M@B}_n\mathrm{H}_n$ possess three π MOs composed by the interesting d-p_z delocalized bonding. And all of the compounds are analogue of benzene, which make those species be good ligands possible. The current work has firmly constituted that transition-metal-centered borane ring are a new class of highly stable and aromatic compounds and our electronic design principle can be used to construct other transition-metal-borane systems.

ACKNOWLEDGMENTS

This work is supported by the National Natural Science Foundation of China (Grant Nos. 21175001 and 21273008) by 211 project of Auhui University. The calculations are carried out on the High-Performance Computing Center of Anhui University. We acknowledge Professor Boldyrev for the AdNDP codes.

[1] N. G. Szwacki, A. Sadrzadeh, and B. I. Yakobson, Phys. Rev. Lett. **98**, 166804 (2007).
[2] J. J. Zhao, L. Wang, F. Y. Li, and Z. F. Chen, J. Phys. Chem. A **114**, 9969 (2010).
[3] E. Oger, N. R. M. Crawford, R. Kelting, P. Weis, M. M. Kappes, and R. Ahlrichs, Angew. Chem., Int. Ed. **46**, 8503 (2007).
[4] L. Wang, J. J. Zhao, F. Y. Li, and Z. F. Chen, Chem. Phys. Lett. **501**, 16 (2010).
[5] F. Y. Tian and Y. X. Wang, J. Chem. Phys. **129**, 024903 (2008).
[6] D. Y. Zubarev and A. I. Boldyrev, J. Comput. Chem. **28**, 251 (2007).
[7] M. Atis, C. Ozdogan, and Z. B. Guvenc, Chin. J. Chem. Phys. **22**, 380 (2009).
[8] L. L. Pan, J. Li, and L. S. Wang, J. Chem. Phys. **129**, 024302 (2008).
[9] H. Tang and S. Ismail-Beigi, Phys. Rev. Lett. **99**, 115501 (2007).
[10] M. P. Johansson, J. Phys. Chem. C **113**, 524 (2009).

[11] J. F. Tian, Z. C. Xu, C. M. Shen, F. Liu, N. S. Xu, and H. J. Gao, Nanoscale **2**, 1375 (2010).
[12] B. Kiran, G. G. Kumar, M. T. Nguyen, A. K. Kandalam, and P. Jena, Inorg. Chem. **48**, 9965 (2009).
[13] M. A. L. Marques and S. Botti, J. Chem. Phys. **123**, 014310 (2005).
[14] B. Kiran, S. Bulusu, H. J. Zhai, S. Yoo, X. C. Zeng, and L. S. Wang, Proc. Natl. Acad. Sci. U.S.A. **102**, 961 (2005).
[15] W. An, S. Bulusu, Y. Gao, and X. C. Zeng, J. Chem. Phys. **124**, 154310 (2006).
[16] L. Rincon, R. Almeida, J. E. Alvarellos, D. Garcia-Aldea, A. Hasmy, and C. Gonzalez, Dalton Trans. **17**, 3328 (2009).
[17] M. I. Eremets, A. G. Gavriliuk, I. A. Trojan, D. A. Dzivenko, and R. Boehler, Nat. Mater. **3**, 558 (2004).
[18] R. R. Zope and T. Baruah, Chem. Phys. Lett. **501**, 193 (2011).
[19] A. Y. Liu, R. R. Zope, and M. R. Pederson, Phys. Rev. B **78**, 155422 (2008).
[20] M. Atis, C. Ozdogan, and Z. B. Guvenc, Int. J. Quantum Chem. **107**, 729 (2007).
[21] M. L. Drummond, V. Meunier, and B. G. Sumpter, J. Phys. Chem. A **111**, 6539 (2007).
[22] D. Prasad and E. D. Jemmis, Phys. Rev. Lett. **100**, 165504 (2008).
[23] T. B. Tai, D. J. Grant, M. T. Nguyen, and D. A. Dixon, J. Phys. Chem. A **114**, 994 (2010).
[24] W. Z. Yao, J. C. Guo, H. G. Lu, and S. D. Lit, J. Phys. Chem. A **113**, 2561 (2009).
[25] M. T. Nguyen, M. H. Matus, V. T. Ngan, D. J. Grant, and D. A. Dixon, J. Phys. Chem. A **113**, 4895 (2009).
[26] S.-D. Li, H.-J. Zhai, and L.-S. Wang, J. Am. Chem. Soc. **130**, 2573 (2008).
[27] H.-J. Zhai, S.-D. Li, and L.-S. Wang, J. Am. Chem. Soc. **129**, 9254 (2007).
[28] M. M. Islam, T. Bredow, and C. Minot, Chem. Phys. Lett. **418**, 565 (2006).
[29] F. Grein, Chem. Phys. Lett. **418**, 100 (2006).
[30] F. Grein, J. Phys. Chem. A **109**, 9270 (2005).
[31] C. H. Chin, A. M. Mebel, and D. Y. Hwang, J. Phys. Chem. A **108**, 473 (2004).
[32] J. Matxain, J. Ugalde, and M. Towler, J. Phys. Chem. A **107**, 10004 (2003).
[33] J. Aihara, J. Phys. Chem. A **105**, 5486 (2001).
[34] T. B. Tai, N. M. Tam, and M. T. Nguyen, Theor. Chem. Acc. **131**, 1241 (2012).
[35] J. Zhang, A. P. Sergeeva, M. Sparta, and A. N. Alexandrova, Angew. Chem., Int. Ed. **51**, 8512 (2012).
[36] G. Martinez-Guajardo, A. P. Sergeeva, A. I. Boldyrev, T. Heine, J. M. Ugalde, and G. Merino, Chem. Commun. **2011**, 6242.
[37] J. O. C. Jimenez-Halla, R. Islas, T. Heine, and G. Merino, Angew. Chem., Int. Ed. **49**, 5668 (2010).
[38] T. B. Tai, N. M. Tam, and M. T. Nguyen, Chem. Phys. Lett. **530**, 71 (2012).
[39] T. B. Tai, A. Ceulemans, and M. T. Nguyen, Chem.-Eur. J. **18**, 4510 (2012).
[40] A. P. Sergeeva, D. Y. Zubarev, H. J. Zhai, A. I. Boldyrev, and L. S. Wang, J. Am. Chem. Soc. **130**, 7244 (2008).
[41] A. P. Sergeeva, Z. A. Piazza, C. Romanescu, W. L. Li, A. I. Boldyrev, and L. S. Wang, J. Am. Chem. Soc. **134**, 18065 (2012).
[42] A. P. Sergeeva, B. B. Averkiev, H. J. Zhai, A. I. Boldyrev, and L. S. Wang, J. Chem. Phys. **134**, 224304 (2011).
[43] C. Romanescu, D. J. Harding, A. Fielicke, and L. S. Wang, J. Chem. Phys. **137**, 014317 (2012).
[44] Z. A. Piazza, W. L. Li, C. Romanescu, A. P. Sergeeva, L. S. Wang, and A. I. Boldyrev, J. Chem. Phys. **136**, 104310 (2012).
[45] Y. Nakagami, N. Y. Suzuki, R. Sekine, T. Matsuura, and J. Aihara, Bull. Chem. Soc. Jpn. **85**, 475 (2012).
[46] W. L. Li, C. Romanescu, T. Jian, and L. S. Wang, J. Am. Chem. Soc. **134**, 13228 (2012).
[47] W. Huang, A. P. Sergeeva, H. J. Zhai, B. B. Averkiev, L. S. Wang, and A. I. Boldyrev, Nat. Chem. **2**, 202 (2010).
[48] B. C. Hikmat, T. Baruah, and R. R. Zope, J. Phys. B **45**, 225101 (2012).
[49] R. Casillas, T. Baruah, and R. R. Zope, Chem. Phys. Lett. **557**, 15 (2013).
[50] L. J. Cheng, J. Chem. Phys. **136**, 104301 (2012).
[51] H.-J. Zhai, A. N. Alexandrova, K. A. Birch, A. I. Boldyrev, and L.-S. Wang, Angew. Chem., Int. Ed. **42**, 6004 (2003).
[52] R. Islas, T. Heine, K. Ito, P. V. R. Schleyer, and G. Merino, J. Am. Chem. Soc. **129**, 14767 (2007).
[53] H. J. Zhai, L. S. Wang, D. Y. Zubarev, and A. I. Boldyrev, J. Phys. Chem. A **110**, 1689 (2006).
[54] H. J. Zhai, C. Q. Miao, S. D. Li, and L. S. Wang, J. Phys. Chem. A **114**, 12155 (2010).
[55] L. Xie, W. L. Li, C. Romanescu, X. Huang, and L. S. Wang, J. Chem. Phys. **138**, 034308 (2013).
[56] C. Romanescu, A. P. Sergeeva, W. L. Li, A. I. Boldyrev, and L. S. Wang, J. Am. Chem. Soc. **133**, 8646 (2011).
[57] C. Romanescu, T. R. Galeev, A. P. Sergeeva, W. L. Li, L. S. Wang, and A. I. Boldyrev, J. Organomet. Chem. **721–722**, 148 (2012).
[58] C. Romanescu, T. R. Galeev, W. L. Li, A. I. Boldyrev, and L. S. Wang, Angew. Chem., Int. Ed. **50**, 9334 (2011).
[59] W. L. Li, C. Romanescu, Z. A. Piazza, and L. S. Wang, Phys. Chem. Chem. Phys. **14**, 13663 (2012).
[60] W. L. Li, C. Romanescu, T. R. Galeev, L. S. Wang, and A. I. Boldyrev, J. Phys. Chem. A **115**, 10391 (2011).
[61] W. L. Li, C. Romanescu, T. R. Galeev, Z. A. Piazza, A. I. Boldyrev, and L. S. Wang, J. Am. Chem. Soc. **134**, 165 (2012).
[62] T. R. Galeev, C. Romanescu, W. L. Li, L. S. Wang, and A. I. Boldyrev, Angew. Chem., Int. Ed. **51**, 2101 (2012).
[63] T. R. Galeev, C. Romanescu, W. L. Li, L. S. Wang, and A. I. Boldyrev, J. Chem. Phys. **135**, 104301 (2011).
[64] A. N. Alexandrova, H. J. Zhai, L. S. Wang, and A. I. Boldyrev, Inorg. Chem. **43**, 3552 (2004).
[65] D. Z. Li, H. G. Lu, and S. D. Li, J. Mol. Model. **18**, 3161 (2012).
[66] D. Z. Li, Q. Chen, Y. B. Wu, H. G. Lu, and S. D. Li, Phys. Chem. Chem. Phys. **14**, 14769 (2012).
[67] Q. Chen and S. D. Li, J. Cluster Sci. **22**, 513 (2011).
[68] H. L. Yu, R. L. Sang, and Y. Y. Wu, J. Phys. Chem. A **113**, 3382 (2009).
[69] L. Li, C. Xu, and L. Cheng, Comput. Theor. Chem. **1021**, 144 (2013).
[70] J. Tao, J. P. Perdew, V. N. Staroverov, and G. E. Scuseria, Phys. Rev. Lett. **91**, 146401 (2003).
[71] Y. Yuan and L. J. Cheng, Int. J. Quantum Chem. **113**, 1264 (2013).
[72] L. F. Li and L. J. Cheng, J. Chem. Phys. **138**, 094312 (2013).
[73] L. Ren, L. J. Cheng, Y. Feng, and X. M. Wang, J. Chem. Phys. **137**, 014309 (2012).
[74] R. Li and L. J. Cheng, Comput. Theor. Chem. **996**, 125 (2012).
[75] Y. Yuan and L. J. Cheng, J. Chem. Phys. **138**, 024301 (2013).
[76] Y. Yuan and L. J. Cheng, J. Chem. Phys. **137**, 044308 (2012).
[77] M. J. Frisch, G. W. Trucks, H. B. Schlegel *et al.*, *Gaussian 09, Revision B.01*, Gaussian, Inc., Wallingford, CT, 2009.
[78] P. Von Rague Schleyer, C. Maerker, A. Dransfeld, H. Jaio, and N. J. R. Van Eikema Hommes, J. Am. Chem. Soc. **118**, 6317 (1996).
[79] D. Y. Zubarev and A. I. Boldyrev, Phys. Chem. Chem. Phys. **10**, 5207 (2008).
[80] T. R. Galeev, B. D. Dunnington, J. R. Schmidt, and A. I. Boldyrev, Phys. Chem. Chem. Phys. **15**, 5022 (2013).
[81] I. A. Popov and A. I. Boldyrev, Comput. Theor. Chem. **1004**, 5 (2013).
[82] J. K. Olson and A. I. Boldyrev, J. Phys. Chem. A **117**, 1614 (2013).
[83] L. J. Cheng, C. D. Ren, X. Z. Zhang, and J. L. Yang, Nanoscale **5**, 1475 (2013).
[84] L. Cheng and J. Yang, J. Chem. Phys. **138**, 141101 (2013).
[85] Z. Pu, K. Ito, P. v. R. Schleyer, and Q.-S. Li, Inorg. Chem. **48**, 10679 (2009).
[86] C. Q. Miao, J. C. Guo, and S. D. Li, Sci. China, Ser. B: Chem. **52**, 900 (2009).
[87] Q. O. Luo, Sci. China, Ser. B: Chem. **51**, 607 (2008).
[88] K. Ito, Z. Pu, Q. S. Li, and P. V. R. Schleyer, Inorg. Chem. **47**, 10906 (2008).
[89] B. B. Averkiev and A. I. Boldyrev, Russ. J. Gen. Chem. **78**, 769 (2008).